RSC Advances

This is an *Accepted Manuscript*, which has been through the Royal Society of Chemistry peer review process and has been accepted for publication.

Accepted Manuscripts are published online shortly after acceptance, before technical editing, formatting and proof reading. Using this free service, authors can make their results available to the community, in citable form, before we publish the edited article. This *Accepted Manuscript* will be replaced by the edited, formatted and paginated article as soon as this is available.

You can find more information about *Accepted Manuscripts* in the Information for Authors.

Please note that technical editing may introduce minor changes to the text and/or graphics, which may alter content. The journal's standard Terms & Conditions and the Ethical guidelines still apply. In no event shall the Royal Society of Chemistry be held responsible for any errors or omissions in this *Accepted Manuscript* or any consequences arising from the use of any information it contains.

ROYAL SOCIETY OF CHEMISTRY

www.rsc.org/advances

Transport Features and Structural Optimization of Solid Lipid Nanoparticles crossing Intestinal Epithelium

Guihong Chai [a, b, +], Yufang Meng [c, +], Shaoqing Chen [a], Fuqiang Hu [a], Yong Gan [b, *], Hong Yuan [a, *].

[a] College of Pharmaceutical Sciences, Zhejiang University, 866 Yuhangtang Road, Hangzhou 310058, China

[b] Shanghai Institute of Materia Medica, Chinese Academy of Sciences, Shanghai 201203, China

[c] Zhejiang Medicine Co., Ltd Xinchang Pharmaceutical Factory, Xinchang 312500, China

[+] These authors contributed equally to this work

Corresponding Author's E-mail: yuanhong70@zju.edu.cn for Hong Yuan and ygan@mail.shcnc.ac.cn for Yong Gan

Abstract: Solid lipid nanoparticles (SLNs) have been used to encapsulate drugs with poor solubility and membrane permeability to improve oral bioavailability. In vitro experiments that determine the SLNs fabrication parameters necessary to achieve satisfactory absorption is important to avoid costly and time-consuming animal experiments. In this study, the Madin-Darby canine kidney (MDCK) cell line was employed to construct a simulated epithelial cell monolayer, and the transport features of SLNs were investigated. Subsequently, SLNs prepared with solid lipid materials with different carbon chain lengths or modified with different amounts of polyethylene glycol monostearate (SA-PEG2000) were used to investigate the relationship between nanoparticle structures and transcytosis efficiency, and the related mechanisms were revealed. Moreover, rats were employed to compare the in vitro and in situ intestinal absorption of these various SLNs. The results demonstrated that the endocytosis and endocellular delivery of SLNs crossing MDCK cell monolayer were vesicle-mediated processes. Studies of the transport capacity of various SLNs across the cell monolayer showed that the transcytosis of SLNs decreased with increasing carbon chain length, and improved with a certain amount of hydrophilic modification (SA-PEG2000, 20%, w/w). The analysis of molecular mechanisms demonstrated that SLNs prepared by solid lipid materials with short carbon chain were inclined to be transcytosed via endoplasmic reticulum (ER)- and Golgi complex-mediated pathways; further, SLNs containing increasingly long carbon chain showed proportionally lower transcytosis by these two organelles. Furthermore, a certain amount of hydrophilic modification can evade transcytosis via the ER- and Golgi complex-mediated pathways for more effective transcytosis. Moreover, the intestinal absorption results were consistent with that found in simulated epithelial cell monolayer. In conclusion, SLNs prepared with solid lipid materials with medium-length carbon chain and surface-modified with a certain amount of hydrophilic modification can transcytosis effectively.

RSC Advances Accepted Manuscript

Keywords: solid lipid nanoparticles; MDCK epithelial cell monolayer; transport features; structural modification; transport difference; in vitro and in situ intestinal absorption.

Introduction

The oral administration of drugs with poor aqueous solubility, poor enzymatic stability and poor membrane permeability is very challenging due to various physiological barriers that exist in the gastrointestinal tract (GIT).[1-3] Nano-sized drug delivery systems are being extensively investigated and show promising potential for oral drug delivery.[4-6] Drugs that are encapsulated in nanocarriers may avoid GIT degradation, diffuse within the mucus, and enhance endocytosis by enterocytes.[7, 8] Solid lipid nanoparticles (SLNs), which are generally prepared using biocompatible and biodegradable solid lipid materials, have gained much attention over the past three decades.[9, 10] SLNs for oral drug delivery have many advantages, e.g., excellent encapsulation of lipophilic drugs, good protection of loaded drugs from degradation, better controlled drug release, and improved transcytosis capacity.[11] Therefore, SLNs have been considered the most promising oral drug delivery system for clinical use.[12, 13]

The performance of SLNs in improving oral drug bioavailability has been widely studied, and the results have indicated that loading drugs into SLNs can markedly increase their absorption efficiency.[12, 13] However, these exciting results have mostly been obtained from animal experiments, such as in vitro and in situ intestinal absorption, or oral bioavailability. These experiments are costly and time-consuming, and the mechanisms related to the SLNs absorption are rarely revealed, because the absorption of the nanocarriers in the animal is complex.[14, 15] Epithelial cell models can be easily manipulated and are an effective tool for investigating the mechanisms of interaction between the nanocarriers and the intestinal epithelium.[16-19] The optimized structure of the SLNs for oral drug delivery may be identified by screening various fabricated SLNs for transcytosis efficiency, and the related transport mechanisms may also be revealed. This may be an effective avenue to obtain the most promising SLNs for oral administration, and the revealed transport mechanisms may aid in the directed design of SLNs.

Transport of SLNs across the intestinal epithelium is a complex process that includes penetrating through the mucus and crossing the intestinal epithelial cell monolayer. Nanocarriers with appropriate properties can easily pass through the mucus overlaying the enterocytes.[20, 21] By contrast, the epithelial cell monolayer is the main barrier to nanoparticle transport.[22, 23] In our previous study, the mechanisms of transport for SLNs prepared with glycerol monostearate were investigated intensively,

RSC Advances Accepted Manuscript

including the mechanisms of SLNs transport across MDCK and Caco-2 cell monolayers.[24, 25] Some valuable findings give us a clear profile of SLNs across the epithelial cell monolayer. The transport efficiency of nanocarriers across intestinal epithelium has been reported to be closely related to the structure of the nanoparticle.[2, 26] In this study, various SLNs with different structures were prepared, and based on previous findings, the mechanisms of their transport across an epithelial cell monolayer were compared. Via these comparisons, a relationship between the structure and the transport efficiency of SLNs was found. Furthermore, the in vitro and in situ intestinal absorption of various SLNs was investigated. From these results, the optimal structure of SLNs with excellent transcytosis efficiency was discovered.

2. Experimental section

2.1. Materials.

Glycerol monopalmitate (GMP) and polyethylene glycol monostearate (SA-PEG2000) were obtained from Tokyo Chemical Industry Co., Ltd. (Japan). Glycerol monostearate (GMS) was obtained from Shanghai Chemical Reagent Co., Ltd. (China). Glycerin monobehenate (GMB) was purchased from Gattefosse (France). Poloxamer 188 was obtained from BASF (Germany). Octadecylamine (ODA) was received from Fluka (U.S.A.). Fluorescein isothiocyanate (FITC), chloropromazine, methyl-β-cyclodextrin (MβCD), brefeldin A, monensin, and nocodazole were purchased from Sigma-Aldrich (St. Louis, MO, U.S.A.). The KeyGEN cell apoptosis DAPI detection kit was provided by Nanjing Keygen Technology Development Co., Ltd. (China). Tissue-Tek® O.C.T. compound was obtained from Sakura Finetek USA, Inc. (U.S.A.). The Madin-Darby canine kidney (MDCK) cell line was obtained from the Institute of Biochemistry and Cell Biology (Shanghai, China). Dulbecco's Modified Eagle's Medium (DMEM, high-glucose), 0.25% trypsin-0.02% EDTA solution, streptomycin, and penicillin were purchased from Gibco BRL (U.S.A.). Fetal bovine serum (FBS) was obtained from Sijiqing Biological Engineering Materials Co., Ltd. All other chemicals were of chromatographic or analytical grade.

2.2. Preparation and characterization of various SLNs

In this study, various SLNs with different structures were fabricated, i.e., the SLNs were prepared using solid lipids with different carbon chain lengths, and the nanoparticles were endowed with different amounts of hydrophilic modification. The solvent diffusion method was used to prepare the various SLNs.[27] As previously reported,[28] ODA-FITC was synthesized to be used as a fluorescence indicator to label the SLNs. The formulations of various SLNs are illustrated in Table 1. In brief,

RSC Advances Accepted Manuscript

ODA-FITC (2.4 mg) and solid lipids (30 mg) were dissolved in 1.5 mL of ethanol at 70°C. Meanwhile, 15 mL of poloxamer 188 solution (0.1%, w/v) was heated to 70°C. Subsequently, the solution of lipids dissolved in ethanol was quickly dispersed into the preheated poloxamer 188 solution by stirring at 400 rpm for 5 min at 70°C. Then, the newly formed droplets of melted lipids were cooled to ambient temperature for solidification. The zeta potential and particle size of various SLNs were detected via dynamic light scattering (DLS) using a Zetasizer analyzer (3000HS, Malvern Instruments Ltd., U.K.). Moreover, the morphology of various SLNs was observed by transmission electron microscopy (TEM, JEM1230, JEOL, Japan). Additionally, Au nanoparticle-loaded SLNs were prepared to trace the transport of SLNs within cells or the cell monolayer according to our previously reported method.[25]

Table 1. Formulations of various SLNs with different structures.

Formulations	GMP	GMS	GMB	SA-PEG2000	ODA-FITC
GMP	24	6			2.4
GMS (GMS-0%PEG)		30			2.4
GMB		6	24		2.4
GMS-20%PEG		24		6	2.4
GMS-40%PEG		18		12	2.4

Note: GMP is glycerol monopalmitate, GMS is glycerol monostearate and GMB is glycerin monobehenate.

2.3. MDCK cell culture and establishment of epithelial cell monolayer

MDCK cells were cultured in DMEM containing 10% fetal bovine serum, 100 U/mL penicillin and streptomycin in a 75 cm^2 plastic flask at 37°C and in a humidified atmosphere (95% relative humidity) containing 5% CO_2. When the cell density reached 80%-90% confluence, MDCK cells were digested with 0.25% trypsin-0.02% EDTA solution and were seeded on polycarbonate filter membranes (pore size: 3 μm, surface area: 1.12 cm^2, Costar Transwell, Millipore Corp., Bedford, MA, U.S.A.). DMEM (0.5 mL) containing 3×10^5 cells was added to the upper chamber of each Transwell device, and cell-free DMEM (1.5 mL) was added to the lower chamber. The medium in the upper and lower chambers was changed every two days. The integrity of the MDCK cell monolayer was verified by measuring the TEER value using a Millicell-ERS volt-ohmmeter (Millipore Co., U.S.A.) after 7 days of culturing. The cell monolayer with a TEER value exceeding 180 $\Omega\bullet cm^2$ was selected for the transcytosis study.

2.4. Transport features of SLNs in MDCK cells

2.4.1. Effects of active transport process and cell membrane fluidity on endocytosis of SLNs

RSC Advances Accepted Manuscript

Before cell culture, 12 mm sterilized circular slides were put into 24-well culture plates. One milliliter of MDCK cells (1×10^5 cells/mL) was seeded in the 24-well plates containing circular slides and cultured for 24h. The cell samples were divided into three groups: the first group was incubated at 37°C with 50 μg/mL of ODA-FITC labelled SLNs (prepared with glycerol monostearate); the second group was incubated at 4°C with 50 μg/mL of ODA-FITC labelled SLNs (prepared with glycerol monostearate); and the third group was pre-treated with 4% paraformaldehyde for 15 min at room temperature, and then the fixing solution was removed, the cells were washed with PBS, and 50 μg/mL of ODA-FITC labelled SLNs (prepared with glycerol monostearate) was added for incubation. All the three groups were incubated for different time (0.5, 1, 2, 4 and 6h). Subsequently, the nanoparticle dispersion was aspirated, and the cell samples were fixed with 4% paraformaldehyde for 15 min at ambient temperature, except for the third group. After that, the fixing solution was removed, the cell samples were washed three times with PBS, and then the cell nucleus was labelled with DAPI for 15 min. After three washes with PBS, the cell samples were sealed for observation with confocal laser scanning microscopy (CLSM).

2.4.2. Effects of SLNs adhesion on cell membrane

The effects of SLNs (prepared with glycerol monostearate) adhesion on the cell membrane were detected by fluorescence recovery after photobleaching (FRAP). First, MDCK cells (1×10^5 cells/mL) were seeded in a glass bottom dish for 24h. Before the FRAP experiment, the MDCK cells were stained with PKH67 Fluorescent Cell Linker (Sigma-Aldrich, St. Louis, MO U.S.A.), which is incorporated into the cell membrane without altering the biological activity of the cells. In brief, 500 μL Diluent C, and then 500 μL of PKH67 dye (4 μM) were added to each well, and the cells were incubated for 10 min at room temperature to label the cell membrane. To stop the staining process, 1 mL of serum was added and incubated for 2 min. After the staining solution was aspirated, the cells were washed with DMEM (containing serum) three times to ensure removal of unbound dye. The stained cell samples were divided into two groups: one group was not treated (control group), and only serum-free culture medium was added; the other group was incubated with 50 μg/mL of SLNs for 30 min at 37°C. For the FRAP experiment, three pictures were taken before photobleaching. Subsequently, a selected region of the cell membrane was bleaching using 100% transmission (Ex: 488 nm). Thereafter, a series of images was taken, and the recovered fluorescence intensity of the bleached region was measured.

2.4.3 Endocytosis of SLNs by MDCK cells

RSC Advances Accepted Manuscript

The endocytosis of SLNs (prepared with glycerol monostearate) by MDCK cells was studied by TEM. First, Au nanoparticle-loaded SLNs were prepared as reported previously to trace the transport of SLNs within MDCK cells. In brief, MDCK cells (1×10^5 cells/mL) were seeded in 6-well plates, and cultured for 24h. Then, the cell samples were divided into two groups: one was untreated (control group), and the other group was incubated with 50 μg/mL of Au nanoparticle-loaded SLNs for 2 h at 37°C. At the end of incubation, the cells were washed with PBS, digested and collected. Subsequently, the cell samples were fixed with 2.5% glutaraldehyde in PBS (0.1 M, pH 7.0) over night. Before the treatment process, the fixed cell sample was washed three times in PBS for 15 min at each step, and then postfixed with 1% OsO_4 in PBS for 2 h and washed another three times with PBS (15 min for each step). Subsequently, the cell samples were first dehydrated with a series of ethanol solutions, and then transferred to absolute acetone. Then, the cell samples were infiltrated and embedded. The embedded cell samples were sectioned, and the ultrathin sections were stained with uranyl acetate and alkaline lead citrate and observed using TEM.

2.5. Transport features of SLNs in MDCK cell monolayer

2.5.1. Effects of SLNs transport on surface morphology of the cell monolayer

The effect of transcytosis of SLNs (prepared with glycerol monostearate) on the surface morphology of the cell monolayer was investigated using a scanning electron microscope (SEM, TM-100, HITACHI, Japan). In brief, MDCK cells were cultured on the insert membrane of a Transwell device for 7 days to form an integral cell monolayer. Then, the cell monolayer samples were divided into two groups: one group was not treated and was only incubated with transport medium (HBSS) for 4 h; the other group was incubated with SLNs for 4 h (100 μg/mL of nanoparticle dispersion was added to the upper compartment of the Transwell device). At the end of the incubation, the cell monolayer, together with the insert membrane, was cut down from the Transwell device. The cell monolayer was washed three times with HBSS, and the cells were then fixed with 2.5% glutaraldehyde in PBS (0.1 M, pH 7.0) over night. Subsequently, the cell monolayer was washed with PBS three times (each step 15 min), postfixed with 1% OsO_4 in PBS for 2 h and washed another three times with PBS. Subsequently, the cell monolayer was first dehydrated in a graded series of ethanol, transferred to a mixture of alcohol and iso-amyl acetate (v:v=1:1) for approximately 30 min, and then transferred to pure iso-amyl acetate overnight. In the end, the cell monolayer was dehydrated with a critical point dryer (Hitachi Model HCP-2) with liquid CO_2. After being coated with gold-palladium, the cell monolayer was observed by using SEM.

RSC Advances Accepted Manuscript

2.5.2. Observation of SLNs transcytosis across MDCK cell monolayer by TEM

The transcytosis of SLNs (prepared with glycerol monostearate) was observed by TEM. In brief, MDCK cells were cultured on the insert membrane (Transwell) to form an integral cell monolayer. Then, the cell monolayer samples were divided into two groups, one of which was incubated with Au nanoparticle-loaded SLNs for 4h of transcytosis. At the end of transcytosis, together with the insert membrane from the Transwell device, the cell monolayer was cut out. The cell membrane was washed three times with PBS, and the subsequent treatment of the cell monolayer was as the same as that described in section 2.4.3. Finally, the transcytosis of Au nanoparticle-loaded SLNs in the MDCK cell monolayer was observed by TEM.

2.6 Comparison of various SLNs across MDCK cell monolayer and their related mechanisms

2.6.1. Transport efficiency of various SLNs endocytosed into or across MDCK cell monolayer

The endocytosis and transcytosis of various SLNs in the MDCK cell monolayer was investigated. In brief, 100 μg/mL of various SLNs (ODA-FITC labelled) was added to the apical side of the cell monolayer (upper compartment of the Transwell device) for 4 h of transport. At the end of the transportation, the transport medium on the apical side or basolateral side, containing various SLNs, was collected. Then, the apical side of the cell monolayer (upper compartment of the Transwell device) was washed three times, and the washing fluid and the originally collected dispersion of SLNs (from the apical side) were combined. The amount of SLNs on the apical side or the basolateral side was measured using a fluorescence spectrophotometer (F-2500, HITACHI Co., Japan). The SLNs endocytosed into the MDCK cell monolayer was defined as the amount of SLNs originally added to the apical side minus the remaining SLNs in the apical side at the end of transportation. The transcytosed SLNs was the amount of SLNs in the basolateral side at the end of experiments.

2.6.2. Related mechanisms of various SLNs endocytosed into or across MDCK cell monolayer

The related mechanisms of various SLNs endocytosed into or across the MDCK cell monolayer were compared. First, the cell monolayer was incubated with different inhibitors (listed in Table 2) for 1h. Then, transport medium on the apical side was replaced with 100 μg/mL of various SLNs (ODA-FITC labelled) containing the same inhibitors for another 4 h of transcytosis. At the end of incubation, the transport medium in the apical side or basolateral side was collected. The apical side of the cell monolayer was then washed three times with HBSS, and the washing fluid and the original dispersion of collected SLNs (from the apical side) was combined. The amount of SLNs on the basolateral side or apical side was measured by fluorescence spectrophotometer.

RSC Advances Accepted Manuscript

Table 2. Different inhibitors used to study the transcytosis of various SLNs.

Inhibitors	Functions	Concentrations
Chloropromazine	Inhibit clathrin-related pathway	30 μM
MβCD	Inhibit lipid raft (or caveolae)-mediated route	2 mM
Brefeldin A	Inhibit transport between ER and Golgi apparatus	25 μg/mL
Monensin	Inhibit transport from Golgi apparatus to cell membrane	32.5 μg/mL
Nocodazole	Inhibit the function of microtubules	6μg/mL

2.7. Intestinal absorption of various SLNs investigated by everted gut sac technique

The intestinal absorption of various SLNs was studied in vitro by using an everted gut sac technique. All animal studies were conducted according to the National Institutes of Health Guide for the Care and Use of Laboratory Animals with the approval of the Scientific Investigation Board of Zhejiang University, Hangzhou, China. Male SD rats (200±20 g body weight) were fasted for 12 h, while water was allowed ad libitum. The rats were sacrificed, and the abdominal cavity was opened with a midline incision to isolate the entire small intestine. The desired intestinal segments were quickly excised and flushed through several times with ice-cold Krebs-Ringer (K-R) culture solution. The intestinal segments were immediately placed in warm (37°C) K-R culture solution, and then gently everted over a glass rod. One side of the intestinal segment (approximately 10 cm) was tied, and the other side was fixed onto an open mouthed device (a plastic bushing). Subsequently, approximately 2 mL of K-R culture solution was injected into the everted intestinal sac, which was balanced in the tube containing K-R culture solution at 37°C for 10 min. At time zero, the balanced everted intestinal sac was suspended in the tube containing 100 μg/mL of various ODA-FITC labelled SLNs (45 mL, diluted with K-R culture solution) and gassed continuously with 95% O_2 and 5% CO_2 while being maintained at 37°C in a Water-bathing Constant Temperature vibrator. At the appropriate time intervals (15, 30, 45, 60, 80, 100 and 120 min), 0.5 mL aliquots of serosal solution were taken from the receiver compartment, and rapidly supplemented with equivalent volumes of fresh K-R culture solution. At the end of the experiment, the width and length of the intestinal segments were measured. The absorption of various SLNs per unit area was calculated as follows: absorption per unit intestinal area (μg/cm^2) = the amount of absorbed SLNs in the sacs (μg)/the intestinal segment area (cm^2).

2.8. Intestinal absorption of various SLNs studied using ligated intestinal loop model

The in situ intestinal absorption of various SLNs was studied by using the ligated intestinal loop model. Male SD rats, fasted for 12h, were anesthetized by an intraperitoneal injection of pentobarbital

RSC Advances Accepted Manuscript

sodium (2%, w/v, 40 mg/kg). The abdominal cavity was cut open, and a 4 cm section of duodenum (jejunum or ileum) was carefully isolated and washed with warm (37°C) K-R culture solution. Then, approximately 100 μg/mL of various ODA-FITC labelled SLNs with equal fluorescence intensity was injected into the selected intestinal loop and ligated at both ends. Subsequently, the treated intestinal loop was put back into the animal's body for another 2 h of absorption. At the end of the absorption, the rats were sacrificed, and the tested intestinal segment was removed, and washed gently with K-R culture solution several times to remove the unabsorbed ODA-FITC labelled SLNs. Then, the treated intestinal segments were embedded in Tissue-Tek® O.C.T. compound and frozen at -80°C overnight. Cryostat sections (5 μm thickness) of the frozen intestinal segment were prepared by using a cryotome (CM1990, LEICA, Germany) maintained at controlled temperature (-20 ± 1°C). The prepared intestinal cryostat section was adsorbed onto the adhesion microscope slides. Subsequently, the sections were stained with DAPI to label the cell nucleus, and then visualized using confocal laser scanning microscopy (CLSM, BX61W1-FV1000, Olympus, Japan).

2.9. Statistics

All data are presented as the mean value ± standard deviation from at least three independent tests. ANOVA was used for statistical analysis, and statistical significance was assigned at $P<0.05$.

3. Results and discussion

3.1. Characterization of various SLNs

To investigate the effects of different SLNs structures on the transport efficiency across the intestinal epithelium, various SLNs with different fabrication parameters were prepared using the solvent diffusion method reported by our group. ODA-FITC was validated to be an effective fluorescence indicator for the SLNs. For the SLNs prepared with solid lipids with short carbon chain, i.e., prepared by GMP, the nanoparticle dispersion was unstable and was disposed to flocculation. Furthermore, the particle size of the SLNs increased with increasing carbon chain length. Therefore, a certain amount (20%, w/w) of solid lipids with medium-length carbon chain (GMS) was added to the SLNs formulations prepared with solid lipids with short (GMP) or long (GMB) carbon chain, which not only improved the stability of SLNs prepared with GMP but also avoided an increase in the particle size of SLNs prepared with GMB. The particle size and zeta potential of various SLNs are shown in Table 3. The results showed that the particle size of various SLNs was approximately 100 nm with a uniform distribution (small polydispersity index value). For SLNs prepared with solid lipids of different carbon chain lengths, the particle size increased slightly with increasing carbon chain length.

RSC Advances Accepted Manuscript

For the SLNs prepared with GMS and different amounts of SA-PEG2000, the particle size decreased slightly. All of the SLNs, had a negative surface charge, and the zeta potential ranged from -20 mV to -30 mV. The morphology of various SLNs was observed by TEM, and the results are illustrated in Figure 1. The micrograph showed that the SLNs prepared with different formulations were spherical nanoparticles, and that all particle sizes were approximately 100 nm, which is consistent with the results of DLS analysis.

Table 3. Particle size and zeta potential of various SLNs.

Formulations	Particle size (nm)	PI	Zeta Potential
GMP	88.6	0.216	-30.56
GMS (GMS-0%PEG)	93.4	0.224	-28.78
GMB	101	0.172	-26.24
GMS-20%PEG	81.8	0.237	-23.38
GMS-40%PEG	77.9	0.156	-21.75

Note: GMP, GMS, GMB refer to the SLNs prepared with glycerol monopalmitate (GMP), glycerol monostearate (GMS) and glycerin monobehenate (GMB), respectively. GMS-20%PEG and GMS-40%PEG represent the SLNs prepared with glycerol monostearate (GMS) and 20% or 40% SA-PEG2000 (w/w), respectively. PI, Polydispersity Index.

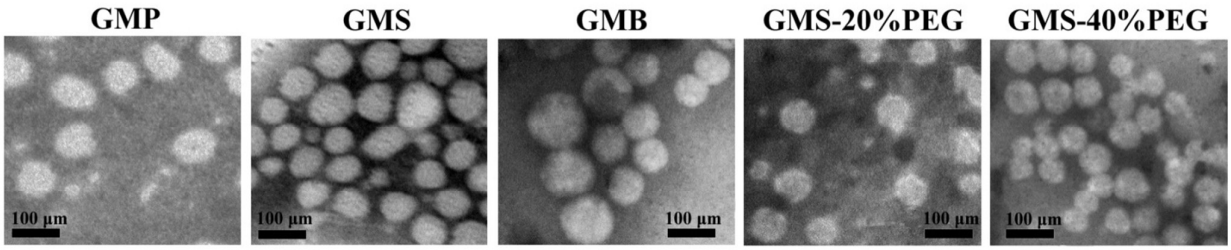

Figure 1. Morphology of various SLNs observed by TEM. GMP, GMS, GMB are the SLNs prepared with glycerol monopalmitate (GMP), glycerol monostearate (GMS) and glycerin monobehenate (GMB), respectively. GMS-20%PEG and GMS-40%PEG are the SLNs prepared with glycerol monostearate (GMS) and 20% or 40% SA-PEG2000 (w/w), respectively.

3.2. Transport features of SLNs in MDCK cells

3.2.1. Effects of active transport processes and cell membrane fluidity on endocytosis of SLNs

In our previous study, a certain amount of SLNs was still found within the MDCK cells when active transport processes was inhibited.[24] To explore the effects of non-active transport process on the transportation of SLNs in MDCK cells, the contribution of passive transport processes and cell membrane fluidity to the transport of SLNs was systematically investigated. Three internalization

RSC Advances Accepted Manuscript

conditions were established: internalization at 37°C or 4°C, and internalization with a fixed cell membrane. In the 4°C condition, the energy-dependent active transport process was inhibited. In the condition of the fixed cell membrane, the fluidity of the cell membrane was restrained. The internalization of SLNs under these three conditions is illustrated in Figure 2. Figure 2A shows the internalization of SLNs at 37°C for 2 h in MDCK cells, and the results indicated that these cells had a better internalization capacity, and that almost none of the internalized SLNs entered the cell nucleus. Figure 2B illustrates the internalization of SLNs under the above mentioned three conditions. In Figure 2B1, which shows internalization at 37°C, the fluorescence intensity in the cells increases with time extended, finally reaching a plateau after 4 h. In Figure 2B2, which shows internalization at 4°C, the corresponding fluorescence intensity at each time point is markedly lower than in the group at 37°C. This indicates that the endocytosis of SLNs was energy-dependent. However, there are still some SLNs within the cells, and these nanoparticles are presumed to have "squeezed" into the cell via membrane bonding and due to the fluidity of the cell membrane. Figure 2B3 shows endocytosis of SLNs under the fixed cell membrane condition, and significantly less fluorescence is seen in the MDCK cells. Fixation of the cell membrane can prevent free mobility of the membrane, and the nanoparticle may only be able to use the membrane fusion to "diffuse" into the cells. For a more clearly displayed difference between endocytosis of SLNs at 4°C and endocytosis with a fixed cell membrane, a magnified picture is shown in Figure 2C. For endocytosis at 4°C, the SLNs can be seen both at the cell membrane and in the cytoplasm (indicated by red arrows). In contrast, when the cell membrane was fixed, most of the SLNs adhered to the cell membrane in ribbon patterns (red arrows indicated). These results indicate that the adherence of SLNs to the cell membrane is a prerequisite for endocytosis, and that the adhered nanoparticles then enter MDCK cells via both active and non-active transport processes, e.g., a membrane fluidity-mediated "squeezing" process or membrane fusion-mediated "diffusion" process.

RSC Advances Accepted Manuscript

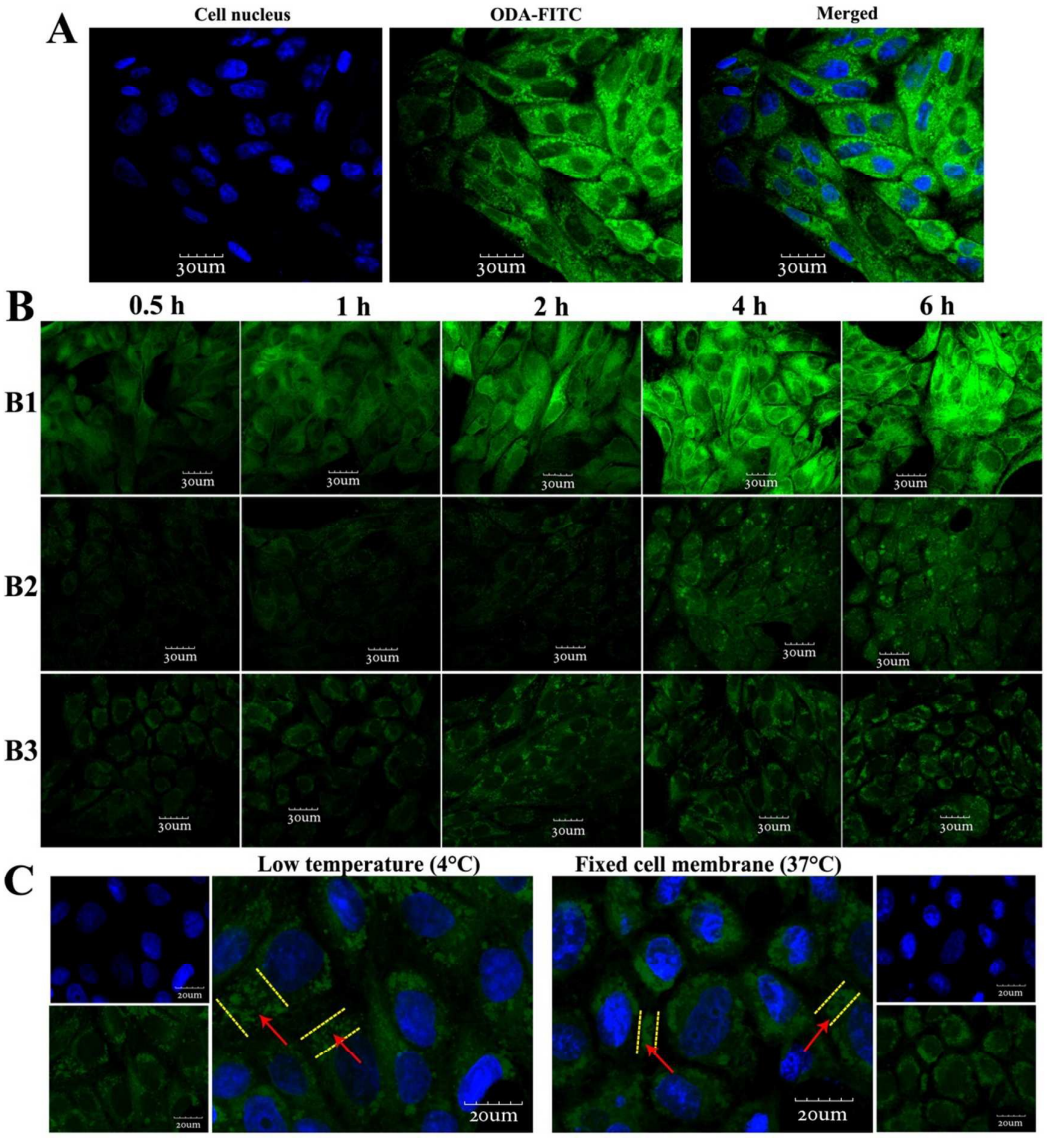

Figure 2. Transport features of SLNs (prepared with glycerol monostearate) in MDCK cells. A. Endocytosis of SLNs (2 h). B. Endocytosis of SLNs under different conditions, where B1 was incubated at 37°C, B2 was incubated at 4°C and B3 was incubated with fixed cell membranes. C. A comparison of the endocytosis of the SLNs under the conditions of 4°C and fixed cell membrane (2 h), and the red arrows show the distribution pattern of SLNs on or within the cells.

3.2.2. Effects of SLNs adhesion on cell membrane

The adhesion of SLNs to the cell membrane has been validated to be a prerequisite for endocytosis. Thus, the effects of SLNs adhesion to the cell membrane was studied by FRAP. The cell membrane was fluorescently labelled with PKH67 (green colour), and the procedure of the experiment, as illustrated in Figure 3A, included pre-bleaching, bleaching, and recovering for different amounts of time after bleaching. The fluorescence intensity of the bleached region was measured before and after

RSC Advances Accepted Manuscript

bleaching during the FRAP procedure. Ten different areas of interest underwent the FRAP process and were integrated to plot a recovery curve (Figure 3B). The results demonstrated that the addition of SLNs significantly decreased the cell membrane fluidity. This may be attributed to the interaction between the cell membrane and the SLNs, and this interaction allows SLNs to enter the cells.

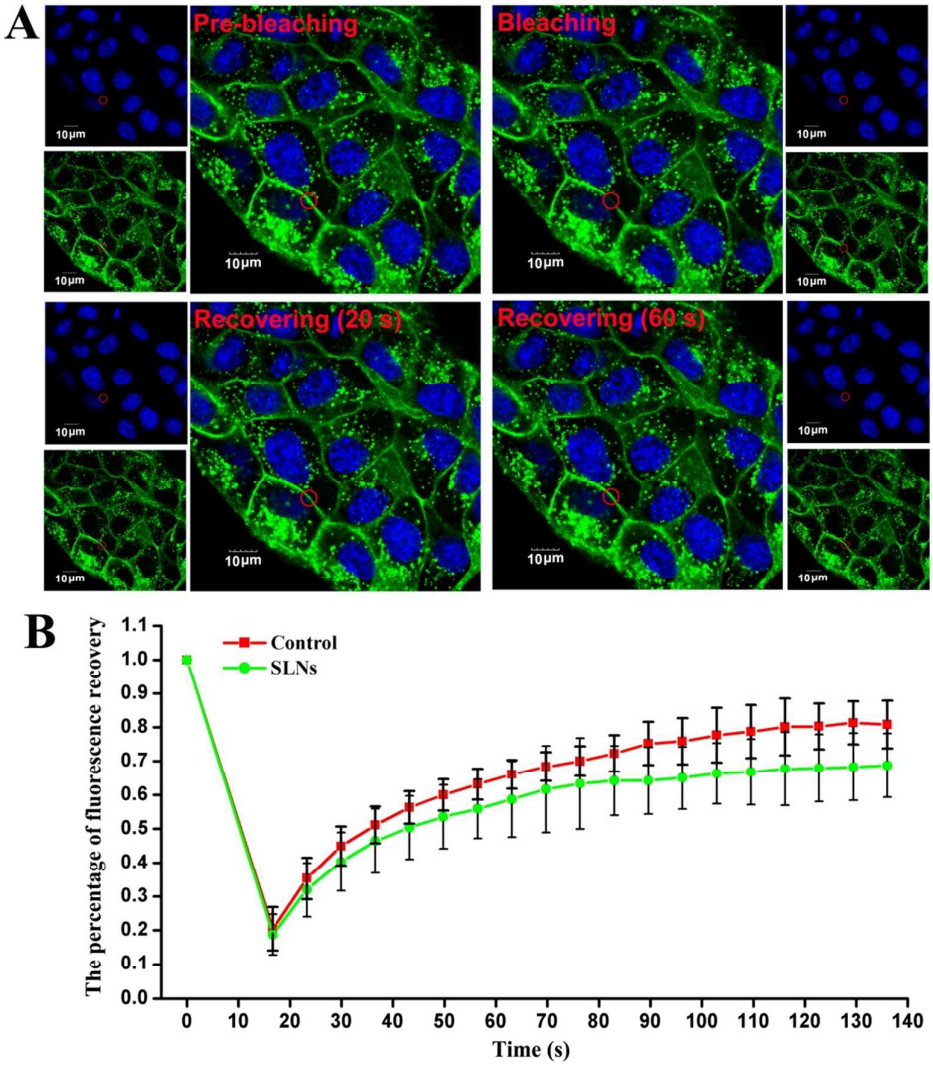

Figure 3. Effects of SLNs adhesion to the cell membrane as detected by FRAP. A. FRAP procedure, in which the red circle on the cell membrane indicates the bleached region. B. Plot of the fluorescence recovery curve from ten regions of interest.

3.2.3. Endocytosis of SLNs by MDCK cells

Endocytosis of SLNs (prepared with glycerol monostearate) was visualized by TEM. Au nanoparticles with a particle size of 5 nm were encapsulated into SLNs to trace the movement of SLNs in cells, and the feasibility of this approach for tracing SLNs has been validated elsewhere.[25] In cell samples that were not incubated with Au nanoparticle-loaded SLNs, no morphology

RSC Advances Accepted Manuscript

corresponding to Au nanoparticle-loaded SLNs was found. By contrast, morphology corresponding to Au nanoparticle-loaded SLNs was found in the cell sample incubated with Au nanoparticle-loaded SLNs. Figure 4 shows the endocytosed SLNs on the cell membrane or within the cells. For SLNs endocytosed on the cell membrane (Figure 4A), the endocytotic structure or the endocytosed Au nanoparticle-loaded SLNs can be seen near the cell membrane (indicated by yellow arrows). For SLNs within the cells (Figure 4B), the endocytosed SLNs were packaged into a vesicle (membrane structure on the exterior of Au nanoparticle-loaded SLNs, indicated by blue arrows). Thus, it can be concluded that the endocytosis or intracellular transport of SLNs is a vesicle-mediated procedure.

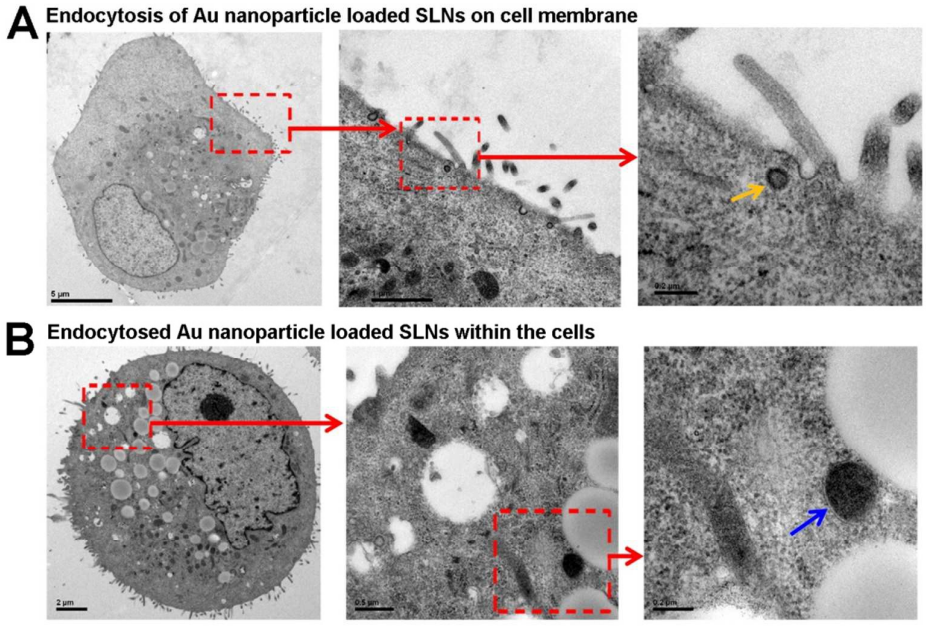

Figure 4. Endocytosis of SLNs (Au nanoparticle loaded) by MDCK cells as viewed by TEM. A. Endocytosis of Au nanoparticle-loaded SLNs on the cell membrane. B. Endocytosed Au nanoparticle-loaded SLNs within the cells. The yellow arrows in A indicate the endocytosed Au nanoparticle-loaded SLNs on the cell membrane, and the blue arrows in B indicate vesicle wrapped Au nanoparticle-loaded SLNs within the cells.

3.3. Transport features of SLNs in MDCK cell monolayer

3.3.1. Effects of SLNs transport on surface morphology of MDCK cell monolayer

SEM was used to study the effects of SLNs transcytosis on cell membrane morphology. As shown in Figure 5A, the addition of SLNs did not have any effects on the morphology of the apical side of the MDCK cell monolayer, with the control group used for comparison. Neither the morphology of tight junctions (TJs) nor the structure of microvilli changed after the transcytosis of SLNs, which indicated that the transcytosis of SLNs was a transcellular process rather than a paracellular one, thus

RSC Advances Accepted Manuscript

confirming that SLNs are safe nanocarriers for oral drug delivery.

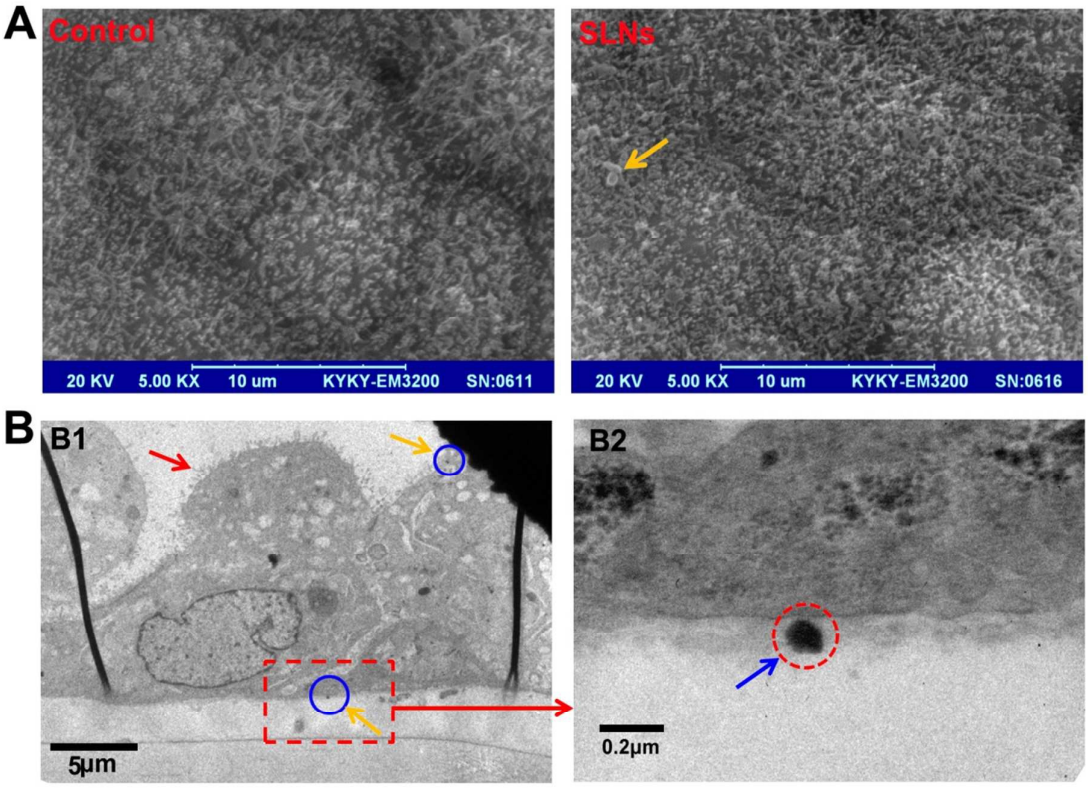

Figure 5. Effects of SLNs transcytosis on the apical side of MDCK cell monolayer viewed by SEM (A) and the transcytosis process of SLNs across the cell monolayer observed by TEM. The yellow arrow in the SLNs sample (Figure 5A) indicates SLNs or SLNs aggregates adhered to the apical side. The blue circle in Figure 5B1 (also indicated by yellow arrows) shows the Au nanoparticle-loaded SLNs beneath the apical membrane and nanoparticles on the outside of the basolateral side (transcytosed SLNs), and the red arrow indicates the microvillus structure. The enlarged picture (Figure 5B2) clearly shows the transcytosed Au nanoparticle-loaded SLNs (indicated by a red circle as well as a blue arrow).

3.3.2. Observation of SLNs transcytosis across MDCK cell monolayer

To visualize the transcytosis (transport from apical side to basolateral side) of SLNs directly, the cell monolayer was prepared for TEM observation after SLNs transport. As noted in previous studies, Au nanoparticle-loaded SLNs were used to trace the transport of the nanoparticle. As shown in Figure 5B1, the structures corresponding to Au nanoparticle loaded SLNs were found on both the apical side and the basolateral side of the MDCK cell monolayer. An enlarged picture of the Au nanoparticle-loaded SLNs on the basolateral side is provided in Figure 5B2, which clearly shows the structure of the Au nanoparticle-loaded SLNs below the basolateral side of the MDCK cell monolayer.

RSC Advances Accepted Manuscript

These results confirmed that the SLNs can be transcytosed to the basolateral side intact.

3.4 Comparison of transcytosis of various SLNs across MDCK cell monolayer and their related mechanisms

The above mentioned results demonstrated the transport features of SLNs across the MDCK cell monolayer via CLSM, SEM and TEM. The aim of elucidating the transport features of SLNs was to use them as a guide to fabricate nanoparticles with excellent transcytosis efficiency. Next, various SLNs were prepared by using solid lipid materials with different carbon chain lengths and by modifying the nanoparticles with different amounts of SA-PEG2000. The transport efficiency and the related mechanisms of these various SLNs were compared.

3.4.1. Transport efficiency of various SLNs endocytosed into or across MDCK cell monolayer

Endocytosis of SLNs into the cell monolayer is the first step of transcytosis. The transport efficiency of various SLNs into the cell monolayer was first compared, and the results are shown in Figure 6A1 and 6B1. For SLNs prepared with solid lipid materials with different carbon chain lengths (Figure 6A1), the results indicated that the amount of SLNs endocytosed into the MDCK cell monolayer decreased with increasing of carbon chain length of solid lipids. For the SLNs (prepared with glycerol monostearate) modified with different amounts of SA-PEG2000 (hydrophilic modification on the surface of the nanoparticles), the endocytosis of SLNs by the cell monolayer increased with a certain amount of SA-PEG2000 modification (20%SA-PEG2000, w/w) (Figure 6B1), and further increases in the amount of modification decreased the amount of endocytosed SLNs. Moreover, the transcytosis efficiency of various SLNs was compared, and the results are displayed in Figure 6A2 and 6B2. For SLNs prepared with solid lipid with different carbon chain lengths, the amount of SLNs transcytosed decreased with increasing of carbon chain length of the solid lipids (Figure 6A2). For the SLNs (prepared with glycerol monostearate) modified with different amounts of SA-PEG2000, a certain amount of SA-PEG2000 modification (20%SA-PEG2000, w/w) increased the transcytosis of SLNs (Figure 6B2), and further increases in the amount of modification decreased the transcytosis efficiency. The underlying causes of these differences in transport between various SLNs were investigated in the following transport mechanism study.

RSC Advances Accepted Manuscript

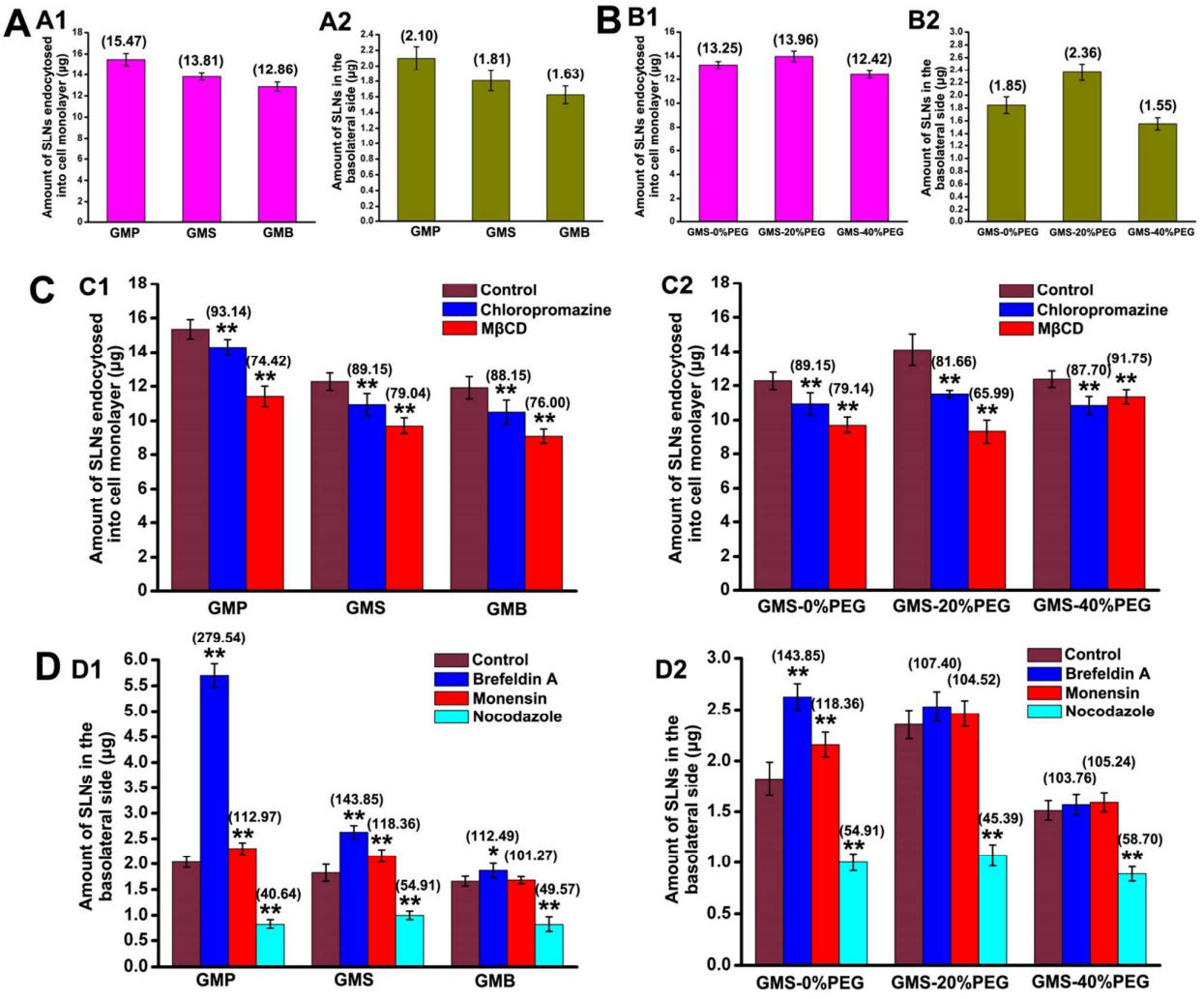

Figure 6. Transport efficiency of various SLNs and comparison of their related mechanisms. A. The efficiency of endocytosis into the cell monolayer (A1) or transcytosis (A2) of SLNs prepared with solid lipids with different carbon chain lengths. B. The efficiency of endocytosis into the cell monolayer (B1) or transcytosis (B2) of SLNs (prepared with glycerol monostearate) modified with different amounts of SA-PEG2000. The figures (A and B) indicate the amount of endocytosed or transcytosed SLNs. C. Mechanistic comparison of various SLNs endocytosed by the cell monolayer. D. Mechanistic comparison of various SLNs transcytosed across the cell monolayer. The figures in brackets indicate the relative percentage of each treatment group (compared with control group). *P<0.05, **P<0.01 compared with control group.

3.4.2. Related mechanisms of various SLNs endocytosed into or across MDCK cell monolayer

The molecular mechanisms of transport of various SLNs across the cell monolayer were studied by inhibiting different endocytotic structures on the apical side as well as endocellular transport routes (Table 2). Chloropromazine [18, 29] and MβCD [17, 30], which inhibit clathrin- and lipid raft (or

RSC Advances Accepted Manuscript

caveolae)-mediated routes, respectively, were added to compare the endocytosis mechanisms of various SLNs into the cell monolayer. Figure 6C shows the results of different mechanisms of endocytosis of various SLNs into MDCK cell monolayer. For SLNs prepared with solid lipids with different carbon chain lengths (Figure 6C1), the endocytosis pathways were not different, i.e., via clathrin- and lipid raft/caveolae-mediated routes. For the SLNs (prepared with glycerol monostearate) modified with different amounts of SA-PEG2000, the endocytosis pathways were also clathrin- and lipid raft/caveolae-mediated routes (Figure 6C2), with some differences in the proportion of SLNs using each pathway. The SLNs modified with a certain amount of SA-PEG2000 (20%, w/w) show significantly greater endocytosis via both routes, whereas reducing or increasing the amount of modification decreased the amount of endocytosis. These results indicate that a certain amount of hydrophilic modification on the surface of the nanoparticles may facilitate the endocytosis of SLNs. Figure 6D shows the different transcytosis mechanisms of various SLNs across the MDCK cell monolayer. As illustrated in Figure 6D1, inhibition of different endocellular transport routes had distinct effects on the amount of transcytosed SLNs prepared with solid lipids with different carbon chain lengths. The addition of brefeldin A, which was used to inhibit transport from the endoplasmic reticulum to the Golgi apparatus,[31, 32] significantly increased the transcytosis of SLNs prepared with solid lipids with short carbon chains, and as the carbon chain length increased, less increase was observed. After adding monensin, which is an inhibitor of transport between the Golgi apparatus and the cell membrane,[16, 33] the proportion of increase in the transcytosis of SLNs did not change significantly, except for the SLNs prepared with solid lipids with long carbon chains. After the addition of nocodazole, an inhibitor of microtubules, the transcytosis of SLNs decreased significantly for the nanoparticles prepared with solid lipids with different carbon chain lengths. For the SLNs (prepared with glycerol monostearate) modified with different amounts of SA-PEG2000, the effects of inhibition of different endocellular transport pathways are shown in Figure 6D2. After the addition of brefeldin A and monensin, inhibitors of the ER- and Golgi apparatus-mediated pathways, the extent to aid the transcytosis of SLNs decreased with the increasing modification with SA-PEG2000, indicating that hydrophilic modification on the surface of SLNs can decrease the proportion of the nanoparticles transported by the ER- and Golgi apparatus-mediated pathways. The addition of nocodazole can also decrease the transcytosis of SLNs modified with different amounts of SA-PEG2000.

The transport mechanism study clearly showed the differences between the various SLNs utilized for endocytosis into or transcytosis across the cell monolayer. For SLNs prepared with solid lipid

RSC Advances Accepted Manuscript

materials with different carbon chain lengths, the nanoparticles prepared with short carbon chains can easily be endocytosed into the cell monolayer compared with SLNs prepared with longer carbon chains. However, a large proportion of the endocytosed SLNs prepared with short carbon chains was transported to the ER and Golgi apparatus, resulting in decreased transcytosis. These further confirmed that the Golgi apparatus- and ER-mediated pathway was important for the transcytosis of SLNs, and the proportion of transport mediated by these two pathways decreased with increasing carbon chain length. From these results, SLNs prepared with medium-length carbon chains are preferentially endocytosed into the cell monolayer with a low proportion of transport mediated by the ER and Golgi apparatus. For SLNs (prepared with glycerol monostearate) modified with different amounts of SA-PEG2000, a certain amount of SA-PEG2000 modification (20%, w/w), can not only increase the endocytosis of SLNs into the cell monolayer but also decrease the proportion of endocytosed SLNs that are transcytosed by the ER- and Golgi apparatus-mediated pathways, resulting in an increased transport efficiency of SLNs across MDCK cell monolayer.

3.5. Intestinal absorption of various SLNs investigated by everted gut sac technique

The everted gut sac technique is a convenient, efficient, and easily handled in vitro method to investigate the intestinal absorption of drugs and their formulations.[34] This technique is often used to study the absorptive capacity, absorption site and mechanisms, and it can more objectively reflect the absorption of drug in the intestines.[35, 36] The intestinal absorption of the various SLNs was investigated using the everted gut sac technique, and the results are shown in Figure 7. After 2 h of experiment, many ODA-FITC labelled SLNs can be seen adhered to the mucus layer on the mucosal membrane of the intestinal segments (data not shown). For the SLNs prepared with solid lipid materials with different carbon chain lengths, the results in Figure 7A show that the intestinal absorption of SLNs via the duodenum, jejunum and ileum was obvious, but the amount of absorbed SLNs was distinct. For total absorption of SLNs via these three intestinal segments, the degree of absorption of SLNs descended in the order of GMP>GMS>GMB, which is in accordance with the results obtained from the cell monolayer. Meanwhile, it can be clearly seen that most SLNs are absorbed in the duodenum. For the SLNs (prepared with glycerol monostearate) modified with different amounts of SA-PEG2000, Figure 7B shows the intestinal absorption of the SLNs. These results demonstrated that a certain amount of hydrophilic modification (20% SA-PEG2000, w/w) significantly increased the absorption of the nanoparticles from these three intestinal segments. Further increases in the amount of modification (40%, w/w) decreased absorption. The performance

RSC Advances Accepted Manuscript

of various SLNs in in vitro intestinal absorption experiments was consistent with that found in the MDCK cell monolayer, further confirming that formulation screening by in vitro experiments using a simulated epithelial cell monolayer was a viable method.

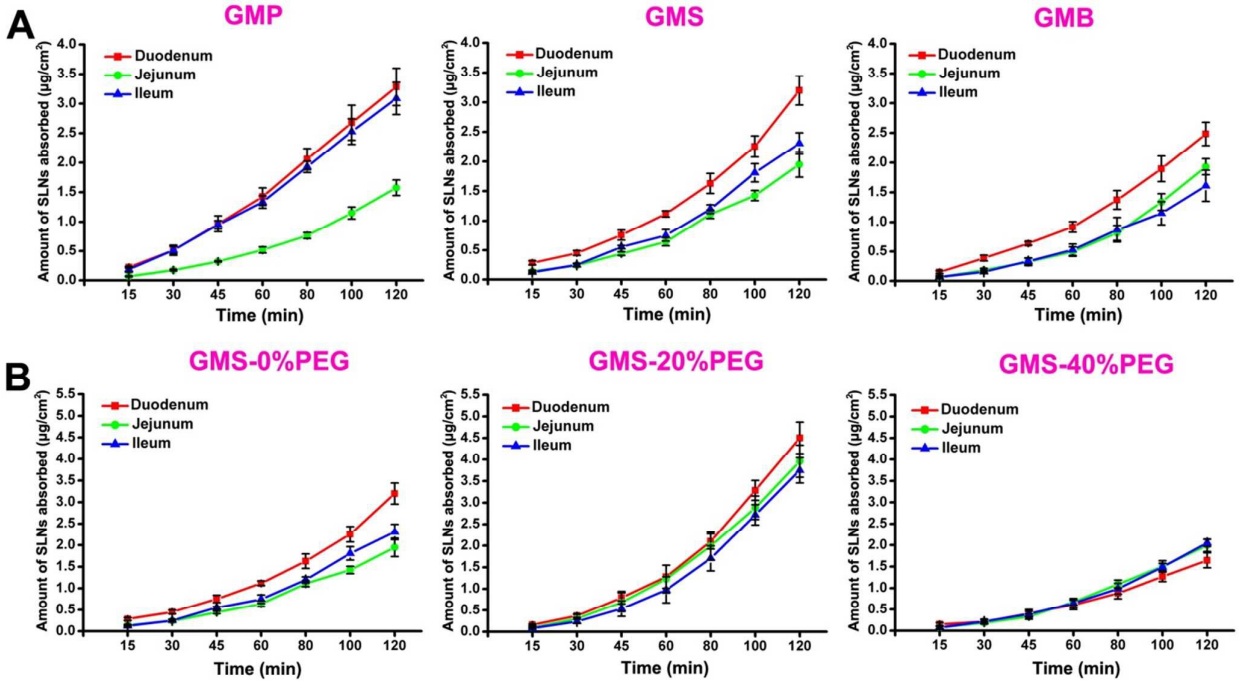

Figure 7. In vitro intestinal absorption of various SLNs investigated by the everted gut sac technique. A. The intestinal absorption of SLNs prepared with solid lipids with different carbon chain lengths. B. The intestinal absorption of SLNs (prepared with glycerol monostearate) modified with different amounts of SA-PEG2000. The absorption of various SLNs is presented as the amount of transcytosed SLNs per unit area of the intestinal segments (duodenum, jejunum and ileum).

3.6. Intestinal absorption of various SLNs studied via ligated intestinal loop model

Although the everted gut sac technique is an effective model for in vitro intestinal absorption of drug or its formulations, it cannot properly mimic aspects of the body environment,[19, 37] such as intestinal peristalsis, rich blood circulation and mucosal metabolic enzymes within the digestive tract. The intestinal loop model (or ligated intestinal loop model) is a common in situ intestinal absorption method for drugs or their formulations.[38, 39] To visualize the absorption of various SLNs in the intestinal villus, double fluorescence labelling with DAPI (nucleus, blue) and ODA-FITC (SLNs, green) were used in the in situ absorption study. When various SLNs are injected into the intestinal loop, the nanoparticles may (1) remain in the intestinal lumen; (2) adhere to mucin fibres or be trapped in mucin; or (3) penetrate through the mucus layer to reach the intestinal epithelium for transcytosis. First, the intestinal absorption of the SLNs (prepared with glycerol monostearate) in different

RSC Advances Accepted Manuscript

intestinal segments (duodenum, jejunum, ileum) was visualized using CLSM, and the results are illustrated in Figure 8B. In the negative control sample (Figure 8A), the autofluorescence of the intestinal segment was weak, and did not affect the comparison of the absorption of SLNs in different intestinal segments. For absorption of the SLNs prepared with glycerol monostearate in different intestinal segments, it can be clearly seen that the duodenum possessed the greatest absorption capability, which is consistent with the finding of the everted gut sac experiments. Next, the intestinal absorption of various SLNs in the dominant intestinal segment (duodenum) was compared. Figure 8C shows the intestinal absorption of SLNs prepared with solid lipids with different carbon chain lengths in the duodenum, and the results demonstrate that with increasing carbon chain length of the solid lipids, the absorption of the SLNs in the intestinal villus decreased. For the absorption of GMP, although the fluorescence in villus was the strongest, the fluorescent intensity of the intestinal wall was lower than that in the GMS sample. These results indicated that SLNs with low carbon chain length can be easily absorbed in the villus, but cannot be transported deeper to the connective tissue beneath the epithelial cells in contrast to the SLNs prepared with solid lipids with medium-length carbon chains. For the SLNs (prepared with glycerol monostearate) modified with different amounts of SA-PEG2000, Figure 8D shows the intestinal absorption of the SLNs in the duodenum. The results indicate that modification with SA-PEG2000 on the surface of SLNs can enhance the permeability of the nanoparticle deep into the mucus, especially when using 20% (w/w) modification. Nanoparticles, such as polystyrene and PLGA nanoparticles, coated with certain Pluronic polymers or polyethylene glycol show lower degrees of mucoadhesion, allowing the rapid penetration of the nanoparticles through the mucus.[40, 41] Our findings indicated that SLNs with a certain amount of hydrophilic modification (SA-PEG2000, 20%, w/w) can significantly increase the penetration of the nanoparticles into mucus, resulting in more nanoparticles reaching the epithelial cell surface for transcytosis. Based on the findings from the MDCK cell monolayer, a certain amount of SA-PEG2000 (20%, w/w) can increase the transcytosis of the SLNs. Therefore, a certain amount of hydrophilic modification can not only enhance the penetration of the nanoparticles through mucus, but also increase the transcytosis of the SLNs across the intestinal epithelial cell monolayer. However, with further increases in the amount of modification with SA-PEG2000 (40%, w/w), most of the SLNs become restrained on the top of the intestinal villus (indicated by red arrows in the GMS-40%PEG sample in Figure 8D), and barely penetrate the mucus. Consequently, it is necessary to optimize the hydrophilic modification of nanoparticles to obtain the best features that can penetrate the mucus easily and facilitate transcytosis

RSC Advances Accepted Manuscript

of the nanoparticles across the epithelial cell monolayer.

The results of the transport mechanism study in the MDCK cell monolayer as well as the in vitro (everted gut sac experiments) and in situ (ligated intestinal loop model) intestinal absorption of the various SLNs indicated that the SLNs prepared with solid lipid with medium-length carbon chain and endowed with a certain amount of hydrophilic modification (e.g., SA-PEG2000, 20%, w/w) on the surface of the nanoparticles can be efficiently transported across the intestinal epithelium.

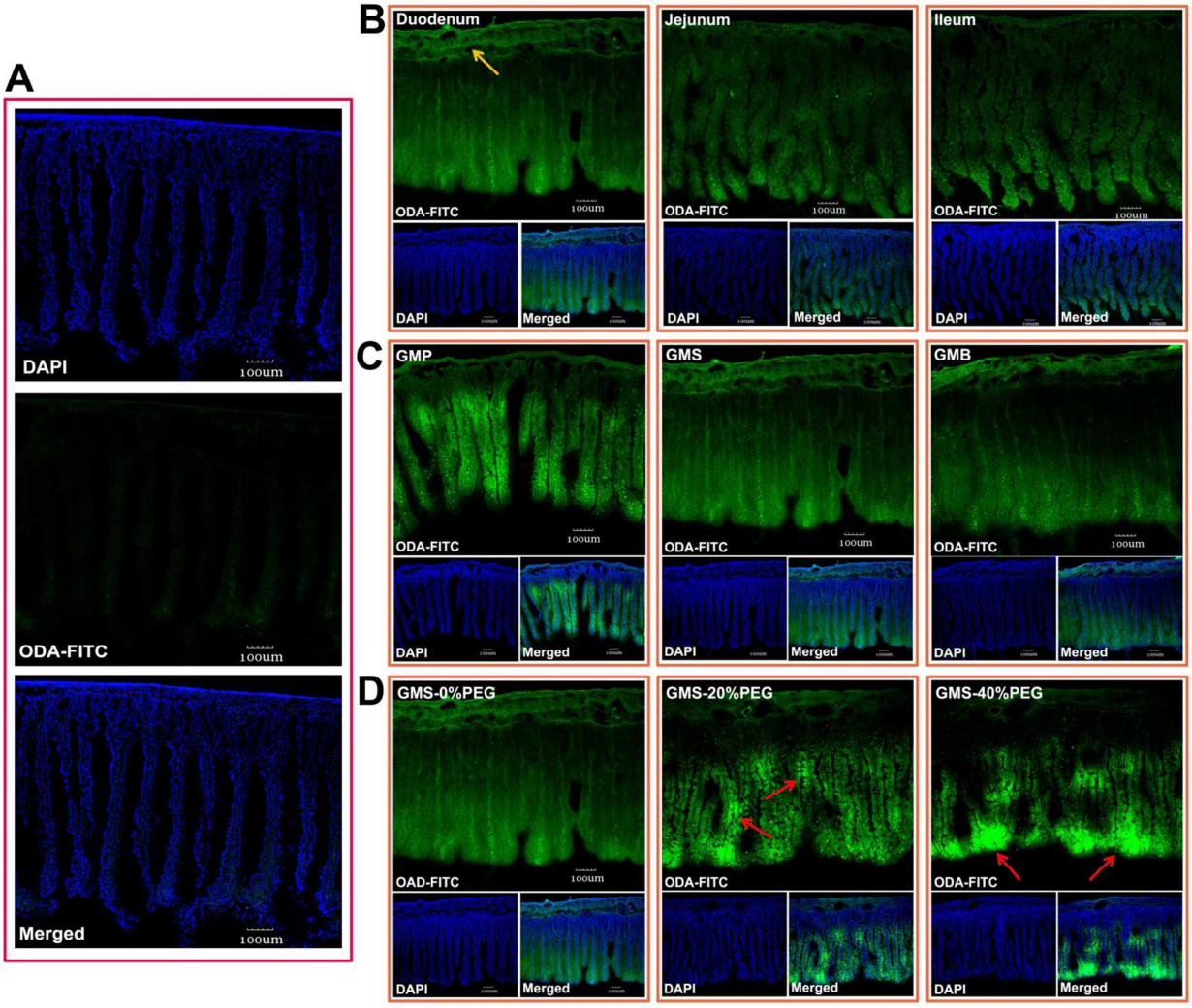

Figure 8. In situ intestinal absorption of various SLNs observed by CLSM. A. Blank intestinal segments (imagined using the same parameters as for the segments treated with ODA-FITC labelled SLNs). B. Absorption of SLNs prepared with glycerol monostearate in different intestinal segments (duodenum, jejunum and ileum). C. Absorption comparison of various SLNs prepared with solid lipids with different carbon chain lengths in the duodenum. D. Absorption comparison of various SLNs (prepared with glycerol monostearate) modified with different amounts of SA-PEG2000 in the duodenum.

RSC Advances Accepted Manuscript

4. Conclusion

Oral delivery of SLNs has been confirmed to be an effective solution to improve the absorption of drugs with poor stability or poor membrane permeability. Here, to effectively screen the optimal properties of SLNs with excellent transport efficiency across the intestinal epithelium, MDCK cell monolayer was employed to screen the optimized SLNs formulations to avoid costly and time-consuming animal experiments. Furthermore, the in vitro and in situ intestinal absorptions of the various SLNs were compared using the everted gut sac and ligated intestinal loop models to validate the viability of the simulative epithelial cell monolayer as a method for screening SLNs formulations. The results showed that the adhesion of SLNs to the cell membrane is a prerequisite of endocytosis, and that the adhesion of SLNs can significantly decrease the cell membrane fluidity. The endocytosis of SLNs and their endocellular transport were vesicle-mediated processes. The transcytosis of SLNs across the MDCK cell monolayer has no effects on the morphology of the apical side, and the SLNs can be transported across the cell monolayer intact. For SLNs prepared with solid lipids with different carbon chain lengths and surface-modified with different amounts of SA-PEG2000, the results of transport efficiency showed that increasing carbon chain length decreased the endocytosis or transcytosis of SLNs, and a certain amount of SA-PEG2000 modification (20%, w/w) increased transcytosis. The transport mechanism study demonstrated that the endocytosis pathways of the various SLNs did not change, just different in the proportion mediated by each pathway. For SLNs prepared with solid lipids with different carbon chain lengths, the endocytosis of the SLNs was mediated by clathrin- or lipid raft/caveolae-related routes, and the proportion via each route did not changed significantly. For the SLNs modified with different amounts of SA-PEG2000, a certain amount hydrophilic modification (20%, w/w) increased the amount of SLNs endocytosed via both above mentioned endocytosis pathways. The transcytosis mechanisms of various SLNs showed that the SLNs prepared with solid lipids with short carbon chain length was predisposed to be transported via ER- and Golgi apparatus-related routes, and with increasing carbon chain length, the proportion transported via these two organelles decreased, resulting in more effective transcytosis of SLNs. For SLNs modified with different amount of SA-PEG2000, the transcytosis of SLNs increased with a certain amount of hydrophilic modification (20%, w/w), and further increases in the amount of modification decreased the transcytosis efficiency. The results of in vitro intestinal absorption demonstrated that the absorption of various SLNs in the duodenum, jejunum and ileum was obvious and that the total absorption of various SLNs was consistent with that found in MDCK cell monolayer

RSC Advances Accepted Manuscript

study. The results of the in situ intestinal absorption study indicated that the duodenum is the most preferable site for SLNs absorption, and that the transport trend of various SLNs was also agreement with that found in the MDCK cell monolayer experiments. Our results demonstrate that SLNs prepared with solid lipids with medium-length carbon chains and surface-modified with a certain amount of hydrophilic modification (e.g., SA-PEG2000, 20%, w/w) can be transported efficiently across the intestinal epithelium. This study provides a novel avenue to screen optimal SLNs formulations via an in vitro simulated epithelial cell monolayer, and may be beneficial for the directed fabrication of SLNs with excellent oral bioavailability.

Acknowledgments

This work was supported by the National Nature Science Foundation of China under Contract No. 81573366, No. 81473144, and No.8127342.

RSC Advances Accepted Manuscript

References

1. A. des Rieux, V. Fievez, M. Garinot, Y.-J. Schneider and V. Préat, *J. Controlled Release*, 2006, **116**, 1-27.

2. E. Roger, F. Lagarce, E. Garcion and J.-P. Benoit, *Nanomedicine*, 2010, **5**, 287-306.

3. L. M. Ensign, R. Cone and J. Hanes, *Adv. Drug Delivery Rev.*, 2012, **64**, 557-570.

4. C. Damge, C. P. Reis and P. Maincent, *Expert Opin. Drug Delivery*, 2008, **5**, 45-68.

5. K. W. Leong and H.-W. Sung, *Adv. Drug Delivery Rev.*, 2013, **6**, 757-758.

6. A. C. Hunter, J. Elsom, P. P. Wibroe and S. M. Moghimi, *Nanomedicine: NBM*, 2012, **8**, S5-S20.

7. P. P. Desai, A. A. Date and V. B. Patravale, *Drug Discovery Today: Technol.*, 2012, **9**, e87-e95.

8. M. J. Alonso, *Biomed. Pharmacother.*, 2004, **58**, 168-172.

9. W. Mehnert and K. Mäder, *Adv. Drug Delivery Rev.*, 2001, **47**, 165-196.

10. J. Wang, J. Chen, N. Ye, Z. Luo, W. Lai, X. Cai and Y. Lin, *Curr. Drug Metab.*, 2012, **13**, 447-456.

11. H. Yuan, C.-Y. Chen, G.-h. Chai, Y.-Z. Du and F.-Q. Hu, *Mol. Pharmaceutics*, 2013, **10**, 1865-1873..

12. R. Pandey, S. Sharma and G. Khuller, *Tuberculosis*, 2005, **85**, 415-420.

13. R. Müller, S. Runge, V. Ravelli, A. Thünemann, W. Mehnert and E. Souto, *Eur. J. Pharm. Biopharm.*, 2008, **68**, 535-544.

14. L. Plapied, N. Duhem, A. des Rieux and V. Préat, *Curr. Opin. Colloid Interface Sci.*, 2011, **16**, 228-237.

15. A. T. Florence and N. Hussain, *Adv. Drug Delivery Rev.*, 2001, **50**, S69-S89.

16. B. He, Z. Jia, W. Du, C. Yu, Y. Fan, W. Dai, L. Yuan, H. Zhang, X. Wang, J. Wang and Q. Zhang, *Biomaterials*, 2013, **34**, 4309-4326.

17. S. Zhao, W. Dai, B. He, J. Wang, Z. He, X. Zhang and Q. Zhang, *J. Controlled Release*, 2012, **158**, 413-423.

18. H. Yuan, L.-J. Lu, Y.-Z. Du and F.-Q. Hu, *Mol. Pharmaceutics*, 2010, **8**, 225-238.

19. J. M. Gamboa and K. W. Leong, *Adv. Drug Delivery Rev.*, 2013, **65**, 800-810.

20. L. M. Ensign, S. Craig, S. J. Soo, C. Richard and H. Justin, *Adv. Biomater.*, 2012, **24**, 3887-3894.

21. B. C. Tang, M. Dawson, S. K. Lai, Y. Y. Wang, J. S. Suk, M. Yang, P. Zeitlin, M. P. Boyle, J. Fu and J. Hanes, *PNAS*, 2009, **106**, 19268-19273.

22. B. He, P. Lin, Z. Jia, W. Du, W. Qu, L. Yuan, W. Dai, H. Zhang, X. Wang and J. Wang, *Biomaterials*, 2013, **34**, 6082-6098.

23. A. T. Florence, *Drug Discovery Today: Technol.*, 2005, **2**, 75-81.

24. G. H. Chai, F. Q. Hu, J. Sun, Y. Z. Du, J. You and H. Yuan, *Mol. Pharmaceutics*, 2014, **11**, 3716-3726.

25. G. H. Chai, Y. Xu, S. Q. Chen, B. Cheng, F. Q. Hu, J. You, Y. Z. Du and H. Yuan, *ACS Appl. Mater. Interfaces*, 2016, **8**, 5929-5940. .

26. T. Jung, W. Kamm, A. Breitenbach, E. Kaiserling, J. Xiao and T. Kissel, *Eur. J. Pharm. Biopharm.*, 2000, **50**, 147-160.

27. F. Hu, H. Yuan, H. Zhang and M. Fang, *Int. J. Pharm.*, 2002, **239**, 121-128.

RSC Advances Accepted Manuscript

28. H. Yuan, J. Chen, Y.-Z. Du, F.-Q. Hu, S. Zeng and H.-L. Zhao, *Colloids Surf., B,*, 2007, **58**, 157-164.

29. Y. Jin, Y. Song, X. Zhu, D. Zhou, C. Chen, Z. Zhang and Y. Huang, *Biomaterials*, 2012, **33**, 1573-1582.

30. X. Li, D. Chen, C. Le, C. Zhu, Y. Gan, L. Hovgaard and M. Yang, *Int. J. Nanomed.*, 2011, **6**, 3151-3162.

31. S. G. Miller, L. Carnell and H. Moore, *J. Cell Biol.*, 1992, **118**, 267-283.

32. W. Fan, D. Xia, Q. Zhu, L. Hu and Y. Gan, *Drug Discov Today*, 2016, DOI: 10.1016/j.drudis.2016.04.007.

33. E. Kuismanen, J. Saraste and R. F. Pettersson, *J. Virol.*, 1985, **55**, 813-822.

34. S. Simovic, Y. Song, T. Nann and T. A. Desai, *Nanomedicine: NBM*, 2015, **11**, 1169-1178.

35. A. Trapani, A. Lopedota, M. Franco, N. Cioffi, E. Ieva, M. Garcia-Fuentes and M. J. Alonso, *Eur. J. Pharm. Biopharm.*, 2010, **75**, 26-32.

36. V. B. Cattani, L. A. Fiel, A. Jäger, E. Jäger, L. M. Colomé, F. Uchoa, V. Stefani, T. Dalla Costa, S. S. Guterres and A. R. Pohlmann, *Eur. J. Pharm. Sci.*, 2010, **39**, 116-124.

37. S. Chakraborty, D. Shukla, B. Mishra and S. Singh, *Eur. J. Pharm. Biopharm.*, 2009, **73**, 1-15.

38. D. Sahana, G. Mittal, V. Bhardwaj and M. Kumar, *J. Pharm. Sci.*, 2008, **97**, 1530-1542.

39. S.-A. Cryan and C. M. O'Driscoll, *Pharm. Res.*, 2003, **20**, 569-575.

40. Y. Cu and W. Saltzman, *Mol. Pharmaceutics*, 2009, **6**, : 173–181.

41. M. Yang, S. K. Lai, Y. Y. Wang, W. Zhong, C. Happe, M. Zhang, J. Fu and D. J. Hanes, *Angew. Chem., Int. Ed. Engl.*, 2011, **123**, 2645–2648

RSC Advances Accepted Manuscript

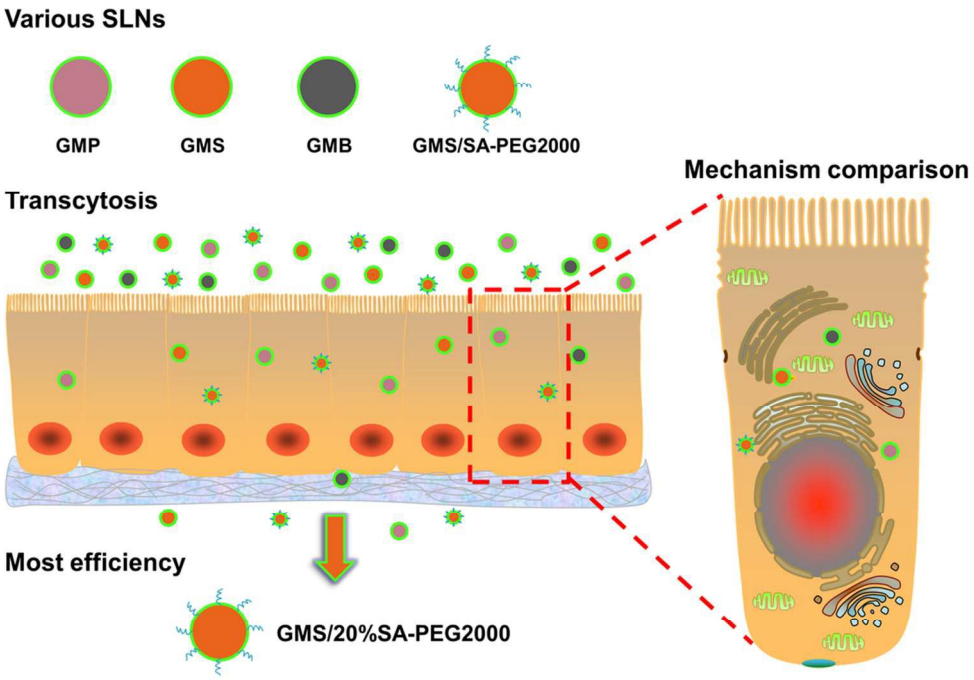

97x73mm (300 x 300 DPI)

RSC Advances Accepted Manuscript